Uni-Planer MIMO Antenna for WLAN and WiMAX Wireless Services

Wan Noor N.W. Marzudi
Research Center of Applied Electromagnetics, Faculty of Electrical and Electronic Engineering, Universiti Tun Hussein Onn Malaysia (UTHM) Batu Pahat, Johor, Malaysia
Email: wannoornajwa [AT] gmail.com

Zuhairiah Zainal Abidin
Research Center of Applied Electromagnetics, Faculty of Electrical and Electronic Engineering, Universiti Tun Hussein Onn Malaysia (UTHM) Batu Pahat, Johor, Malaysia
Email: zuhairia [AT] uthm.edu.my

Siti Zarina Mohd. Muji
Faculty of Electrical and Electronic Engineering, Universiti Tun Hussein Onn Malaysia, 86400 Parit Raja, Batu Pahat, Johor. Malaysia
Email: szarina [AT] uthm.edu.my

Adham Maan Salah
School of Engineering and Informatics, University of Bradford, Bradford, BD7 1DP, UK
Email: a.m.s.saleh [AT] bradford.ac.uk

Issa Tamer Elfergani
Instituto de Telecomunicações, Aveiro, Portugal
Email: i.t.e.elfergani [AT] av.it.pt

Raed A. Abd-Alhameed
School of Engineering and Informatics, University of Bradford, Bradford, BD7 1DP, UK
Email: r.a.a.abd [AT] bradford.ac.uk

James M. Noras
School of Engineering and Informatics, University of Bradford, Bradford, BD7 1DP, UK
Email: j.m.noras [AT] bradford.ac.uk

***Abstract*:** A dual-wideband MIMO antenna for WLAN/Wi-Fi/WiMAX services is presented. This design comprises of two radiating G-shaped slotted patch antennas placed symmetrically. The isolation is enhanced by introducing a neutralization line and a defected ground plane. The impedance bandwidth is improved by adding a stub in the feeding line. The size of the overall antenna is 35 × 35 × 1.026 mm^3. The antenna impedance bandwidth is 12.34% between 2.28–2.58 GHz and 68.49% between 3.00–5.88 GHz; the S_{11} is improved to be less than -10 dB and the isolation is greater than -12 dB. The performance characteristics of the present MIMO design are examined in terms of the S-parameters, envelope correlation coefficient (ECC), capacity loss, channel capacity, total active reflection coefficient (TARC), radiation patterns and power gains. Finally, the results of such investigations confirm that this design is suitable for WLAN and WiMAX systems.

Indexing Terms: MIMO antenna, ECC, TARC, WLAN, WiMAX.

I. INTRODUCTION

Considering the unprecedented evolution of wireless communication system, this has raised demands for higher data rate and larger capacity in wireless applications such as Bluetooth, Wi-Fi, LTE, WLAN and WiMAX. MIMO technology lies in incorporating multiple antennas at the transmitting and receiving ends, this is one promising approach to achieve higher data rates without consuming extra power in rich scattering environments [1, 2]. However, as they are fitted closely together on confined substrates, the isolation between MIMO elements becomes lower, whereas to achieve the best performance, the isolation must be as high as possible. Several methods have been proposed to enhance the isolation.

Methods reported include using parasitic elements [3, 4], T-shaped junctions and branches [5, 6], defected ground structures (DGS) [7], stubs [8] and neutralization lines (NL) [9-13]. This latter approach improves the isolation between the antenna elements in a small spacing by introducing effective inductance to neutralize the capacitance of the antenna elements [12]. The present paper proposes a dual band G-shaped slotted MIMO antenna structure, with a neutralization line and a slot etched on the antennas' ground. This antenna is an improvement on a previous design [14], with a size reduction of about 16%. Measurements show the antenna has come up with an impedance bandwidth from 2.28–2.58 GHz / 3.00–5.88 GHz, with S_{11} < -10 dB and S_{21} < - 12 dB.

II. THE ANTENNA LAYOUT AND PROCEDURE

Fig. 1 illustrates the geometry of the present MIMO antenna, this antenna was printed over the RT5880LZ substrate that has a relative permittivity of 1.96 and a height of 1.026 mm. The present design was made up of two identical G-shaped slotted antenna elements. This antenna has some similarities with authors' previous design [15]. Two identical defected areas with rectangular shape are made on the ground with the purpose of broadening the antenna bandwidth. A wavelength of about 0.144λ at 2.4 GHz was choosing to be the space between the antenna elements. An approach of adding the neutralization strip is exploited to enhance the isolation at 2.4 GHz. On other hand, to mitigate the coupling at 3.5 GHz, an etched rectangular slot is generated in the middle of the ground. Moreover, to further improve the impedance matching, a stub is added on the feeding line as depicted in Fig. 1. The present design occupies a compact volume of 35 × 35 × 1.026 mm^3.

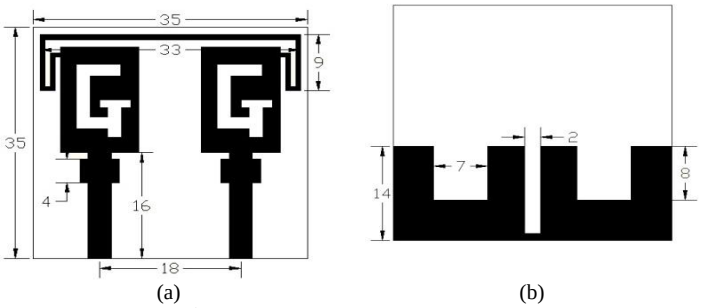

(a) (b)

Figure 1: Geometry of the proposed antenna (dimensions in mm). (a) Front view; (b) Back view.

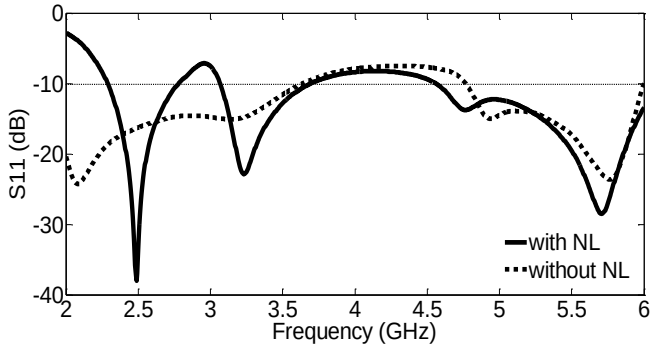

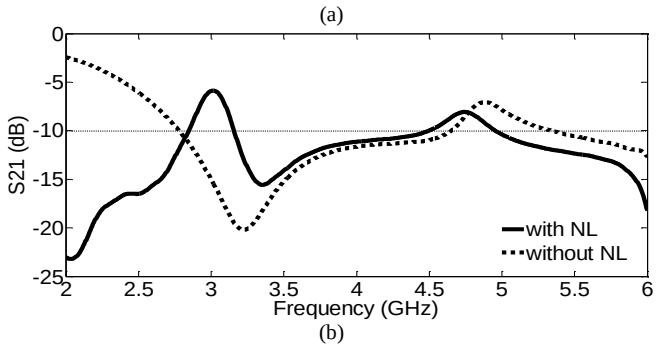

Figure 2: Simulated S-Parameter with and without neutralization line. (a) Reflection coefficient S_{11}; (b) Transmission coefficient S_{21}.

III. PARAMETRIC STUDY

To further understand the effect of the neutralization line, rectangular slot and stub on the performance of the antenna, parametric studies were intensively implemented.

A. The Infulences of the Neutralization Line on the S-Parameters of the Antenna

To analysis the contributions of the neutralization line, the computed S-Parameters of the antenna in the case of the inclusion and exclusion of the neutralization line are depicted in Fig. 2. Fig 2(b) demonstrates that the isolation between the radiating elements in the absence of the neutralization line is low at 2–2.776 GHz and 4.656–5.34 GHz. Generally speaking, the isolation is usually low at the lower frequency band, while it is higher at the upper frequency band. By introducing the neutralization strip, the mutual coupling at 2.4 GHz is found less than -15 dB, but higher at 2.848–3.156 GHz and 4.496–4.952 GHz.

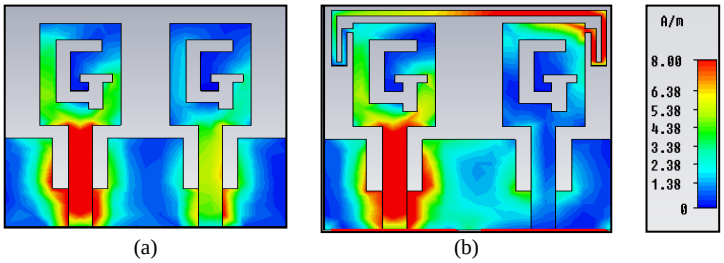

Figure 3: The current distribution at 2.4 GHz. (a) without neutralization line; (b) with neutralization line.

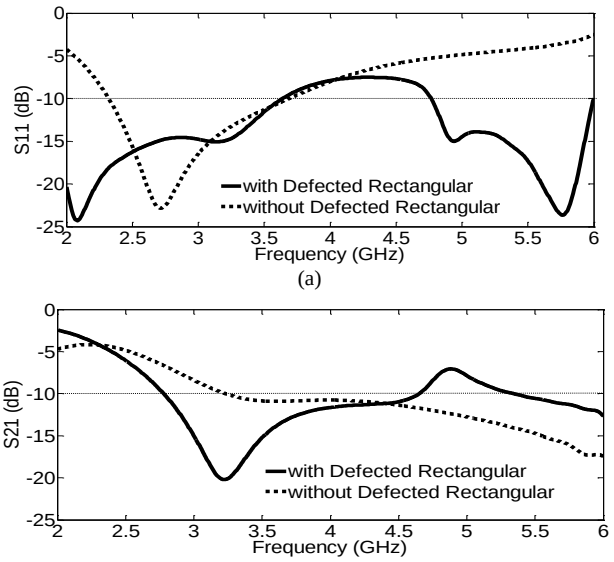

(b)

Figure 4: Simulated S-parameters with and without the rectangular slot. (a) Reflection coefficient, S_{11}; (b) Transmission coefficient, S_{21}.

To realize the contributions of the neutralization line, the surface currents of the proposed design in the case of including and excluding the neutralization strip at 2.4 GHz are presented in Fig. 3. This is accomplished by exciting port 1, while at the same time port 2 should be terminated with a matching load. Fig. 3(a) demonstrates the current induced in the feeding line of port 2 is strong at 2.4 GHz in the case of not including the neutralization strip. When the neutralization line is inserted, as in Fig. 3(b), this introduces a new current path. With the purpose of improving the coupling, another additional coupling was generated, which in turns can compensate the original coupling [16].

B. The Impacts of the rectangular slot on S-parameters of the antenna

The effective technique of using rectangular slot is constructed as depicted in Fig. 1(b), in which it is contributed in mitigating the mutual coupling of the antenna [17]. A comparison of the antenna performance in both cases (with and without the slot) is indicated in Fig. 4(a). From Fig. 4(b), it is noted that by introducing the slot, the isolation is enhanced to better than -12 dB at 2.848–3.156 GHz and 4.496–4.952 GHz. Moreover, a huge enhancement of around of 15.83% and 61.89% in the antenna bandwidth is met, in which a frequency range from 2.164–2.536 GHz and 3.164–6 GHz was also correspondingly covered as shown in Fig. 4(a).

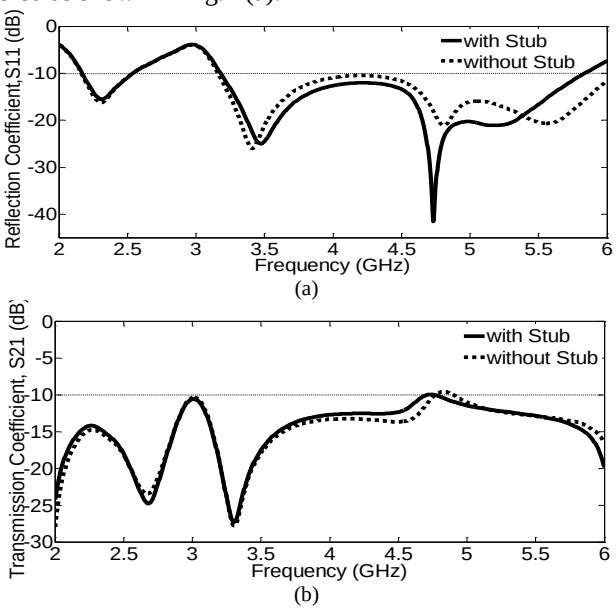

(b)

Figure 5: Simulated S-parameters with and without neutralization line. (a) Reflection coefficient, S11; (b) Transmission coefficient, S21.

C. The Effects of the Stub on S-parameters of the Antenna

A stub with overall dimensions of 5 × 3.5 mm is printed on the feeding strip near to radiating element in order to improve antenna impedance matching [18]. The S-parameters with and without the printed stub are shown in Fig. 5. The introduction of the stub improves the impedance matching at the upper frequencies but decreases the end of the higher frequency band. Two bands has been achieved from (2.28–2.58) GHz and (2.88–5.88) GHz < -10 dB with an isolation less than < -12 dB, in which covers both WLAN and WiMAX systems.

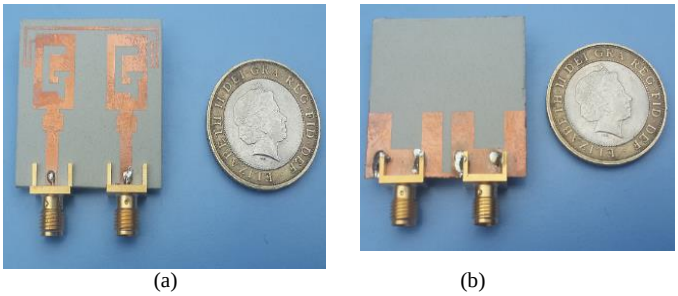

(a) (b)

Figure 6: Prototype of the proposed antenna, (a) Front view; (b) Back view.

IV. RESULTS AND DISCUSSIONS

To verify the computed findings, the antenna based on the configuration in Fig. 1 was manufactured and validated. The manufactured design is displayed in Fig. 6. The S-parameters were measured using a Rohde & Schwarz ZVB14 vector network analyser (VNA). The anechoic chamber is used to measure the radiation patterns. Based on the measurements, the performances of the MIMO antenna were analysed. Details of S-parameters, radiation patterns, current distributions, antenna gain, and diversity performance are profoundly addressed in the next sections.

The calculated and measured outcomes of the S-parameters have been compared as explained in Fig. 7. It is obviously seen that there is a fair agreement between them. Even though, there are some variances due to the measurement tolerances. Two different bandwidths are appeared, which are (2.28–2.58) GHz and (3–5.88) GHz, with a reflection coefficient S_{11} < -10 dB and mutual coupling S_{21} < -12 dB. These bands cover the following wireless services; LTE2300, LTE 2600, Bluetooth, Wi-Fi, WLAN and WiMAX.

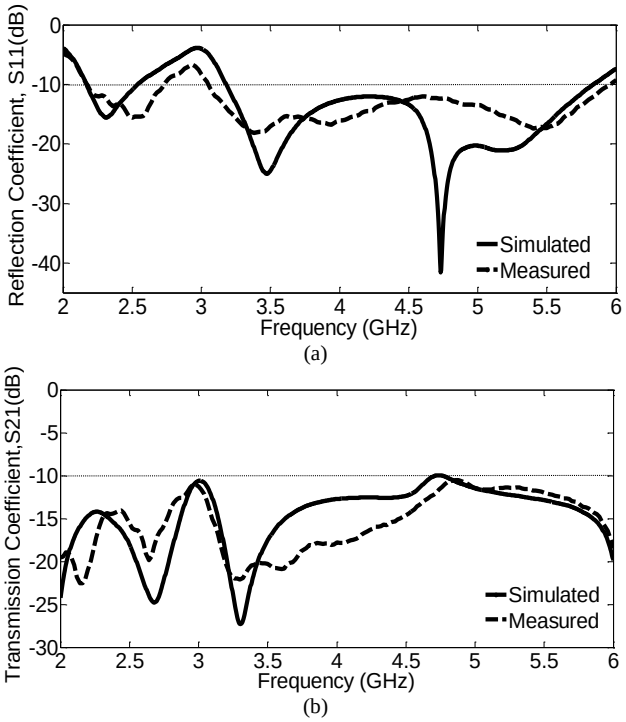

Figure 7: Comparison of S-parameters using simulated and measured results. (a) Reflection coefficient, S_{11}; (b) Transmission coefficient, S_{21}.

The far-fields patterns of the fabricated design were tested at four selected frequencies, 2.4, 3.5, 5.5, and 5.8 GHz, as depicted in Fig. 8. These patterns were tested in the two planes of XZ and YZ , in the case of excitation of port 1 and termination of port 2, and showed a stable omnidirectional pattern at all frequencies.

For possible applications as a MIMO/diversity antenna, the envelope correlation coefficient (ECC) is paramount factor. Generally, there are two different methods to evaluate the ECC of array antennas, firstly, the ECC can be obtained from the far-field radiation pattern method [1, 19] and secondly it may be accomplished from the S-parameters from the antenna system approach [20]. For the antenna proposed here, the envelope correlation was obtained from S-parameter measurements, as in the following expression [20]:

$$\rho_e = \frac{|S_{*11}S_{12}+S_{*21}S_{22}|}{(1-|S_{11}|^2-|S_{21}|^2)\,(1-|S_{22}|^2-|S_{12}|^2)} \quad (1)$$

The measured ECC is shown in Fig. 9, with ρ_e measured as less than 0.005, significantly less than 0.5, the requirement for diversity [21].

Generally, by increasing the number of antennas, this will lead to enhancing the channel capacity of the MIMO system. Whilst, a loss in the channel capacity may be occur when the uncorrelated Rayleigh-fading is present and/or exist.

For 2 × 2 MIMO systems, the correlation matrix can be used to obtain the channel capacity loss [22]. The simplified channel capacity loss may be calculated by utilizing the next equation [10, 23]:

$$C_{loss} = -log_2 \det(\varphi^R) \quad (2)$$

where φ^R is the receiving antenna correlation matrix:

$$\varphi^R = \begin{bmatrix} \rho_{11} & \rho_{12} \\ \rho_{21} & \rho_{22} \end{bmatrix}$$

with $\rho_{ii} = \left(1 - \left(|S_{ii}|^2 + |S_{ij}|^2\right)\right)$

and $\rho_{ij} = -\left(S_{ii}^* S_{ij} + S_{ji}^* S_{jj}\right)$, for i , j = 1 or 2.

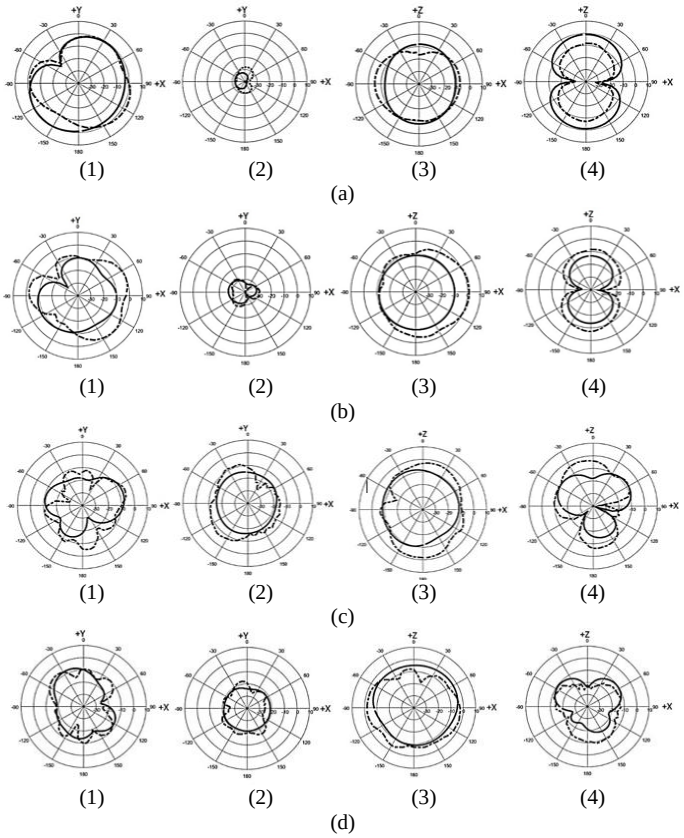

Figure 8: Simulated and measured radiation patterns of the proposed antenna for two planes [(1 and 2) y-x plane and (3 and 4) z-x plane] at (a) 2.4 GHz, (b) 3.5 GHz, (c) 5.5 GHz and (d) 5.8 GHz . Port 1 is excited and port 2 is terminated. "____" simulated results, "_ _ _" measured results, '1 and 3' co-polar components and "2 and 4" cross-polar components.

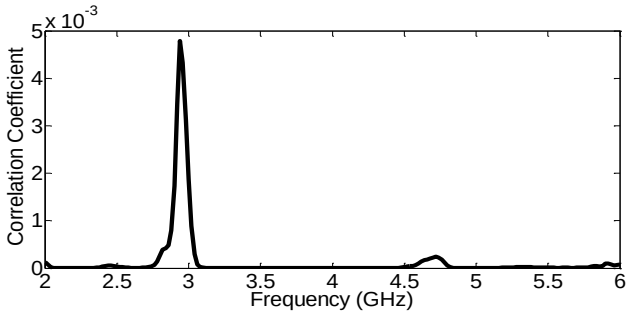

Figure 9: Measured Envelope Correlation Coefficient.

The TARC may be described as the square root of the ratio of a) the total power available at all the ports minus the radiated power to b) the total available power [24]. The TARC can be evaluated by using the following two port network formula [10]:

$$\tau_a^t = \sqrt{\frac{\left((|S_{11}+S_{12}e^{j\theta}|^2)+(|S_{21}+S_{22}e^{j\theta}|^2)\right)}{2}} \qquad (3)$$

The computed and measured TARC and capacity loss of the present design are compared and explained in Fig. 10. In neither case the capacity loss does exceed 0.6 bps/Hz. The discrepancy between calculated and practical results is attributable to fabrication and measurement tolerances. The characteristics of this proposed MIMO antenna in several wireless application frequency bands are summarized in Table I, where it obviously appears that the antenna has low loss of capacity and ECC.

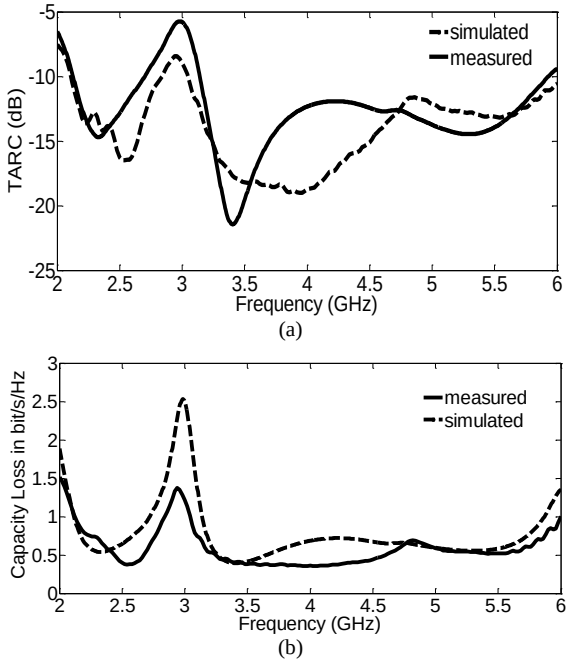

Figure 10: Simulated and measured MIMO characteristics of the proposed antenna. (a) TARC; (b) Capacity loss.

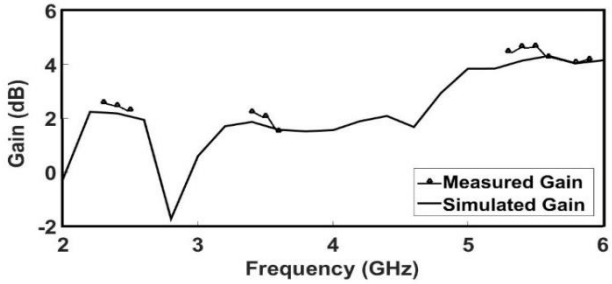

Figure 11: Comparison between simulated and measured gain.

Table 1: MIMO Characteristic Performances.

MIMO Parameter	at 2.4 GHz	at 3.5 GHz	at 5.2 GHz	at 5.8 GHz
ECC (10^{-5})	3.36	0.026	1.32	3.23
Capacity Loss (bit/s/Hz)	0.561	0.382	0.543	0.687
TARC (dB)	-13.84	-18.2	-12.69	-11.9

The theoretical and measured power gains of the antenna are plotted in Fig.11. The measured gain shows good agreement with simulated result. In the upper band the maximum deviation is less than 0.5 dB.

Table 2: Substrate Material.

Substrate Material	Rogers RT5880	FR-4
Dielectric permittivity, ε_r	1.96	4.4
Tangent Loss	0.0019	0.025
Thickness, h	1.026 mm	1.6 mm

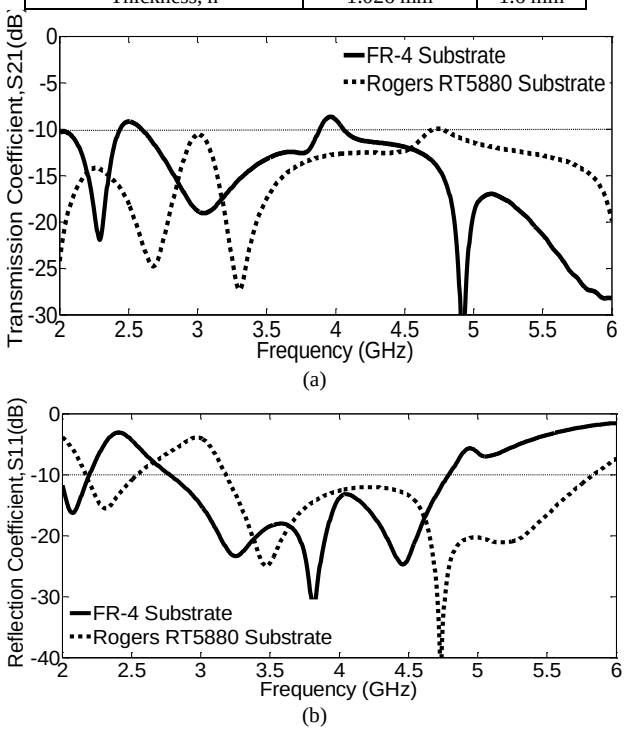

Figure 12: Simulated S-parameters using different substrates. (a) Reflection coefficient, S11; (b) Transmission coefficient, S21.

V. ANTENNA PERFORMANCES USING DIFFERENT SUBSTRATES

Theoretically, the influence of the substrate may affect the antenna performances [25]. Therefore, the effects of the substrate parameters such as; thickness, dielectric permittivity and loss tangent are investigated to determine the loss and

bandwidth of the antenna by comparing two different conventional substrate materials, Rogers RT5880 LZ and FR-4 epoxy. Table II shows the details of these two substrates.
Simulated S-parameters using FR-4 and Rogers substrates are compared in Fig. 12. It is noticeable that the low value of dielectric permittivity ε_r enhances the obtainable bandwidth, as proven in [26], and gives the best return loss.

Table 3: Antenna Performances

Material	Bandwidth (GHz)	Frequency (GHz)	Mutual Coupling (dB)
FR-4	2-2.196 2.776-4.778	2.4	-11.6
		3.5	-13.24
		5.5	-17.04
		5.8	-26.98
ROGERS RT5880	2.28 – 2.58 2.88 – 5.88	2.4	-15.67
		3.5	-17.54
		5.5	-12.12
		5.8	-14.41

Measured S-parameters using both FR-4 and Rogers substrates are indicated in Fig. 13: a slight frequency shift takes place between the computed and measured outcomes, due to measurement setup tolerances. The performances in terms of antenna bandwidth, mutual coupling and return loss using the two substrates are stated and detailed in Table III. One can note that Rogers substrate gives a better impedance bandwidth. The relative bandwidths for FR-4 are 9.34% (2–2.196) GHz and 53% (2.776–4.778) GHz, whilst for Rogers 5880; relative bandwidths of 12.34% and 68.49% at 2.28–2.58 GHz and 2.88–5.88 GHz respectively are obtained.

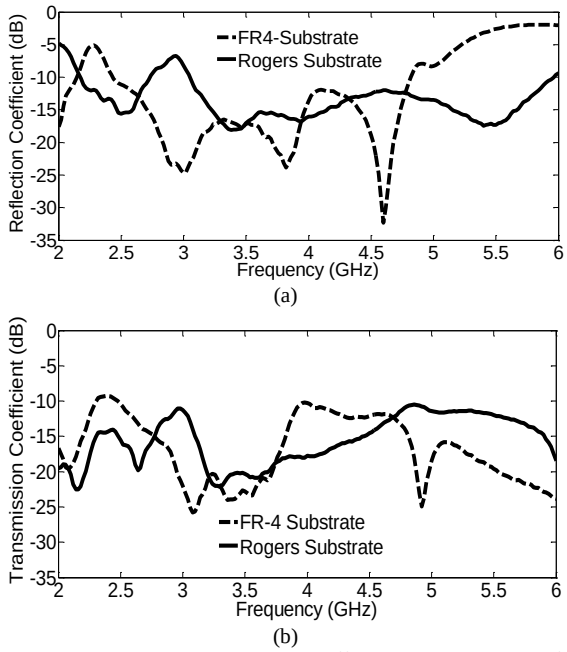

Figure 13: Simulated S-parameters using different substrates: (a) Reflection coefficient, S11; (b) Transmission coefficient, S21.

VI. CONCLUSION

Uni-Planer Multi-Band MIMO Antenna with G shape has been designed and presented covering the WLAN and the WiMAX service bands. The antenna achieves bandwidths of 12.34% from 2.28 to 2.58 GHz and of 68.49% from 3 to 5.88 GHz with a promising isolation better than 12 dB. Measurements show good agreement with simulation results.

REFERENCES

1. Vaughan, R.G. and Andersen, J.B., *Antenna diversity in mobile communications.* Vehicular Technology, IEEE Transactions on, 1987. **36**(4): pp. 149-172.
2. Foschini, G.J. and Gans, M.J., *On limits of wireless communications in a fading environment when using multiple antennas.* Wireless personal communications, 1998. **6**(3): pp. 311-335.
3. Addaci, R., Diallo, A., Luxey, C., Le Thuc, P., Staraj, R., *Dual-band WLAN diversity antenna system with high port-to-port isolation.* Antennas and Wireless Propagation Letters, IEEE, 2012. 11: pp. 244-247.
4. X. b. Sun and M. Y. Cao, "Low mutual coupling antenna array for WLAN application," in *Electronics Letters*, vol. 53, no. 6, pp. 368-370, 3 16 2017.
5. Liu, X.L., Wang Z.D, Yin X.Z and Wang J.H., *Closely spaced dual band-notched UWB antenna for MIMO applications.* Progress In Electromagnetics Research C, 2014. **46**: pp. 109-116.
6. Qin, H. and Liu, Y.-F., *Compact Dual-Band MIMO Antenna with High Port Isolation for WLAN Applications.* Progress In Electromagnetics Research C, 2014. 49: pp. 97-104.
7. Sharmaa, P. and Khanb, T., *A Compact MIMO Antenna with DGS Structure.* International Journal of Current Engineering and Technology, 2013. **3**(3): pp. 780-782.
8. Zhao, H., Zhang, F., Wang, C and Liang. J, *A Compact UWB Diversity Antenna*. International Journal of Antennas and Propagation, 2014. 2014.
9. W. Marzudi, Abidin, Z., Yue, M., and Abd-Alhameed, R.A., *Two-Elements Crescent Shaped Printed Antenna for Wireless Applications*, in Advanced Computer and Communication Engineering Technology. vol. 315, ed: Springer International Publishing, 2015, pp. 195-203
10. Su, S.-W., Lee, C.-T., and Chang, F.-S., *Printed MIMO-antenna system using neutralization-line technique for wireless USB-dongle applications.* Antennas and Propagation, IEEE Transactions on, 2012. 60(2): pp. 456-463.
11. Wang, Y. and Du, Z., *A Wideband Printed Dual-Antenna with Three Neutralization Lines for Mobile Terminals.* IEEE Transactions on Antennas and Propagation, March 2014. 62(No 3).
12. S. Zhang and G. F. Pedersen, "Mutual Coupling Reduction for UWB MIMO Antennas With a Wideband Neutralization Line," in *IEEE Antennas and Wireless Propagation Letters*, vol. 15, no. , pp. 166-169, 2016.
13. Huang, J.-H., Chang, W.-J., and Jou, C.F., *Dual-Band MIMO Antenna with High Isolation Application by Using Neutralizing Line.* Progress In Electromagnetics Research Letters, 2014. 48: pp. 15-19.
14. Marzudi, W.N.N.W., Abidin, Z.Z, Muji, S.Z.M, Yue, Ma and Abd-Alhameed, R.A, *Wideband G-Shaped Slotted Printed Monopole Antenna for WLAN and WiMAX Applications.* International Journal on Electrical and Informatic Engineering, September 2014. 6(3): pp. 596-605.
15. Marzudi, W.N.W and Abidin Z.Z, *Dual Wideband G-Shaped Slotted Printed Monopole Antenna for WLAN and WiMAX Application.* RF and Microwave Conference (RFM), 2013 IEEE International: pp. 225-227.
16. Ban, Y., Chen, Z., Kang, K., and Li. J., *Decouped hepta band antenna array for WWAN/LTE Smartphone.* IEEE Antennas and Wireless Propagation Letters, 2014. 13:pp. 999-1002.

17. Ren, J., Mi, D., and Yin, Y.-Z., *Compact Ultrawideband MIMO Antenna with WLAN/UWB Bands Coverage.* Progress In Electromagnetics Research C, 2014. **50**: pp. 121-129.
18. See, T.S. and Chen, Z.N., *An ultrawideband diversity antenna.* Antennas and Propagation, IEEE Transactions on, 2009. **57**(6): pp. 1597-1605.
19. Bhatti, R.A., Choi, J.-H., and Park, S.-O., *Quad-band MIMO antenna array for portable wireless communications terminals.* Antennas and Wireless Propagation Letters, IEEE, 2009. 8: pp. 129-132.
20. Xiong, L. and Gao, P., C*ompact Dual-Band Printed Diversity Antenna For Wimax/Wlan Applications*. Progress In Electromagnetics Research C, 2012. 32.
21. Li, J.-F., Chu, Q.-X., and Huang, T.-G., *A compact wideband MIMO antenna with two novel bent slits.* Antennas and Propagation, IEEE Transactions on, 2012. 60(2): pp. 482-489.
22. Chae, S.H., Oh, S.-K., and Park, S.-O., *Analysis of mutual coupling, correlations, and TARC in WiBro MIMO array antenna.* IEEE Antennas and Wireless Propagation Letters, 2007. 6: pp. 122-125.
23. See, C.H., Abd-Alhameed R.A., Abidin Z.Z, McEwan N.J, Excell, P.S. *Wideband printed MIMO/diversity monopole antenna for WiFi/WiMAX applications.* Antennas and Propagation, IEEE Transactions on, 2012. 60(4): pp. 2028-2035.
24. Manteghi, M. and Rahmat-Samii, Y., *Multiport characteristics of a wide-band cavity backed annular patch antenna for multipolarization operations.* Antennas and Propagation, IEEE Transactions on, 2005. **53**(1): pp. 466-474.
25. Schaubert, D.H., Pozar, D.M., and Adrian, A., *Effect of microstrip antenna substrate thickness and permittivity: comparison of theories with experiment.* Antennas and Propagation, IEEE Transactions on, 1989. **37**(6): pp. 677-682.
26. Waterhouse, R., *Microstrip Patch Antennas: A Designer's Guide*. 2003: Springer.